Mechanistic Insight into the Polymerization of Butadiene by "Ligand-Free" Polybutadienyl−Nickel(II) Complexes: Computational Assignment of the True Structure of the Resting State†

Sven Tobisch*,‡ and Rudolf Taube§

University of St Andrews, School of Chemistry, Purdie Building, North Haugh, St Andrews, KY15 9ST, United Kingdom, and Fuchsienweg 17, 06118 Halle/Saale, Germany

Received December 3, 2007

Summary: DFT calculations have unveiled the true structure of the catalyst resting state of butadiene polymerization by "ligand-free" polybutadienyl−nickel(II) complexes and have rationalized the origin of its stability. A detailed view of the chain growth process is presented that assists in the assignment of spectroscopically observable intermediates.

The metal-catalyzed stereoselective polymerization of butadiene has been the subject of considerable research efforts in both industry and academia.[1–4] The mechanism has been examined most thoroughly for Ni(II) π-allyl complexes.[5–9] Comprehensive experimental investigations by Taube have culminated in the proposed two-channel reaction model for the allylnickel(II)-catalyzed polymerization of butadiene.[3] The formally cationic "ligand-free" polybutadienyl−Ni^{II} compound $[Ni(C_{12}H_{19})]X$ (**A**) has been discovered as a highly active, cis-1,4-regulating initiator.[3,10,11] The structure of *syn*-**A** has been unequivocally established by NMR spectroscopy, conductivity measurements, and X-ray structural analysis.[10a,c,e,h] High-resolution ^1H NMR spectroscopy furthermore disclosed that the η^3:η^2:η^2-C_{12} chain attached to nickel bears an identical conformation in solution.[10f]

Scheme 1.[12]

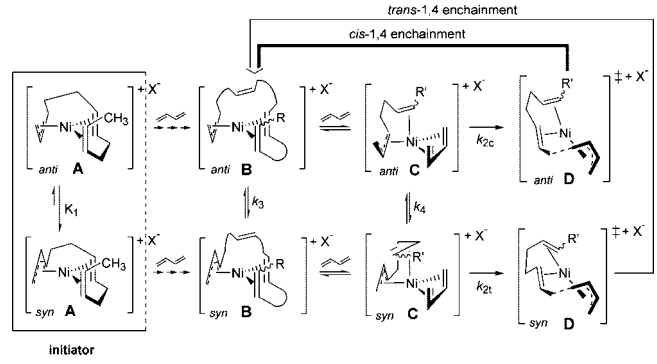

Scheme 1[12] depicts the proposed chain growth mechanism with **A** as the initiator.[3,10] This mechanism has precedence in allylnickel(II) chemistry and is in consonance with the anti-cis and syn-trans correlation.[3] Kinetic studies revealed that the polymerization rate is first-order in [catalyst] and [butadiene],[10d,g] thereby implicating the TS structure **D**. All essential aspects of the mechanism have been confirmed, and a more in-depth understanding has been provided by a detailed computational examination.[13] In light of the apparent equilibrium between the syn and anti forms of initiator **A**, which is on the side of *syn*-**A**,[10a] it was originally believed that the analogue *syn*-**B** is the most stable form of the propagating species. DFT calculations revealed unfavorable kinetics for isomerization of the terminal butenyl group in **B** or **C**.[13] This led us previously to suggest *anti*-**C** as the catalyst resting state for the cis-1,4-generating channel.

In recent low-temperature experiments the Brookhart group isolated the $[(anti\text{-}\eta^3\text{:}\eta^2\text{:}\eta^2\text{-}C_{15}H_{23})-Ni^{II}]^+$ intermediate **X1** by treating an in situ generated cationic allyl−nickel(II) complex with 3 equiv of butadiene (Scheme 2).[14] It is worth noting that the reported X-ray structure of **X1**[14] bears great similarity to *anti*-**B**, featuring a four-coordinate square-planar Ni^{II} center

* To whom correspondence should be addressed. E-mail: st40@st-andrews.ac.uk.

† Dedicated to Prof. Dr Dr h.c. mult. W. A. Herrmann on the occasion of his 60th birthday.

‡ University of St Andrews.

§ Fuchsienweg 17, 06118 Halle/Saale.

(1) Durand, J. P.; Dawans, F.; Teyssie, P. *J. Polym. Sci., Part A* **1970**, *8*, 979.

(2) Porri, L.; Giarrusso, A.; Ricci, G. *Prog. Polym. Sci.* **1991**, *16*, 405.

(3) Taube, R.; Sylvester, G. In *Applied Homogeneous Catalysis with Organometallic Complexes*; Cornils, B., Herrmann, W. A., Eds.; VCH: Weinheim, Germany, 1996, pp 280–318..

(4) Thiele, S. K.-H.; Wilson, D. R. *J. Macromol. Sci., Part C: Polym. Rev.* **2003**, *C43*, 581.

(5) Kormer, V. A.; Babitskii, B. D.; Lobach, M. I. *Adv. Chem. Ser.* **1969**, *91*, 306.

(6) Harrod, J. F.; Wallace, L. R. *Macromolecules* **1969**, *2*, 449.

(7) Dolgoplosk, B. A. *Sov. Sci. Rev., Sect. B* **1980**, *2*, 203.

(8) Hadjiandeou, P.; Julemont, M.; Teyssie, M. *Macromolecules* **1984**, *17*, 2455.

(9) Taube, R.; Schmidt, U. *Z. Chem.* **1977**, *17*, 349.

(10) (a) Taube, R.; Böhme, P.; Gehrke, J.-P. *J. Organomet. Chem.* **1990**, *399*, 327. (b) Taube, R.; Gehrke, J.-P.; Böhme, P.; Scherzer, K. *J. Organomet. Chem.* **1991**, *410*, 403. (c) Taube, R.; Wache, S. *J. Organomet. Chem.* **1992**, *428*, 431. (d) Taube, R.; Langlotz, J. *Makromol. Chem.* **1993**, *194*, 705. (e) Taube, R.; Wache, S.; Sieler, J.; Kempe, R. *J. Organomet. Chem.* **1993**, *456*, 131. (f) Wache, S.; Taube, R. *J. Organomet. Chem.* **1993**, *456*, 137. (g) Taube, R.; Wache, S.; Kehlen, H. *J. Mol. Catal. A: Chem.* **1995**, *97*, 21. (h) Taube, R.; Langlotz, J.; Sieler, J.; Gelbrich, Th.; Tittes; K, *J. Organomet. Chem.* **2000**, *597*, 92.

(11) The $[Ni(C_{12}H_{29})]X$ complex with the weakly coordinating $B(C_6H_3(CF_3)_2)_4$ counterion is a highly active initiator ($N_t \approx 12\,000$ mol of C_4H_6 (mol of Ni)$^{-1}$ h^{-1} at 25 °C in benzene) that yields a PBD of predominant cis-1,4-structure (93% cis-1,4, 4% trans-1,4, and 3% 1,2-enchainment).[10c]

(12) The curved lines in *syn*-**B** and *anti*-**B** indicate some uncertainty regarding which of the double bonds of the polybutadienyl chain actually coordinate at the Ni center. The reversible arrows connecting *syn*-/*anti*-**B** and *syn*-/*anti*-**C** describe the existing equilibrium, without elaborating further on its kinetics.

(13) (a) Tobisch, S.; Taube, R. *Organometallics* **1999**, *18*, 5204. (b) Tobisch, S. *Acc. Chem. Res.* **2002**, *35*, 96.

(14) O'Connor, A. R.; White, P. S.; Brookhart, M. *J. Am. Chem. Soc.* **2007**, *129*, 4142.

(15) Tao, J.; Perdew, J. P.; Staroverov, V. N.; Scuseria, G. E. *Phys. Rev. Lett.* **2003**, *91*, 146401.

10.1021/om701214u CCC: $40.75
Publication on Web 04/24/2008

Scheme 2

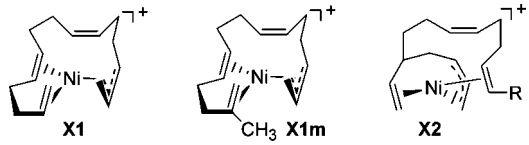

spanned by the *anti*-η^3-butenyl terminal group and the second and third cis C=C bonds, while the first axial cis π-bond is noncoordinated. The analogue **X1m**, obtained from a methallyl−nickel(II) compound, exhibits the same coordination pattern of the chelating polybutadienyl chain (Scheme 2). This type of polybutadienyl−Ni^{II} compound proved to be not the most stable form under polymerization conditions, and NMR experiments identified instead a vinyl-coordinated species (as originating from a rare 1,2-insertion) as the resting state.[14] The suggested structure **X2** is shown in Scheme 2.[14]

Inspired by Brookhart's work,[14] we communicate herein the computational assessment of all relevant elementary events of the *cis*-1,4 polybutadiene-generating channel by employing the DFT method as an established and predictive means to aid mechanistic understanding. Our previous computational study examined exclusively 1,4-enchainment by using an appropriate, but somewhat downsized, structural model. The present DFT survey (TPSS[15]/SDD[16]+TZVP[17])[18] employs [(*anti*-η^3-$C_{15}H_{22}R$)-Ni^{II}(*cis*-η^4-C_4H_6)]$^+$ (R = CH_3) as a realistic catalyst model that mimics the active butadiene π-complex under polymerization conditions and explores both regular cis-1,4- and rare 1,2-insertion to be followed by up to three regular events. We concentrate herein exclusively on the most accessible of the several stereochemical pathways and performed an extensive DFT simulation of configurationally and conformationally different polybutadienyl−Ni assemblies. The full account of stereochemical pathways, together with a detailed elucidation of the mechanism of stereoregulation, can be found elsewhere.[13] The mechanistic conclusions derived are based on computed Gibbs free-energy profiles.

We start by probing whether the first or second C=C bond of the growing chain, acting as the coordinated fifth ligand, is most effective in smoothing the insertion profile (Figure 1). *cis*-Butadiene coordinates preferably in a bidentate fashion upon axial association of the first π-bond (**2a**), while complexation of the second π-bond forces butadiene into a η^2 mode (**2b**). The associated TS structures **3a**,**b**, both of which constitute the *cis*-butadiene insertion into the *anti*-η^3-butenyl group (π-allyl insertion mechanism),[3,13] show similar characteristics and decay initially into **1b**. The transient polybutadienyl−Ni^{II} species **1b** has the chelating chain associated through its first axial and second equatorial π-bonds and readily transmutes into the more stable **1a**. Interestingly, **1a** is congruent with **X1** without the attached growing chain.[19] Comparison of the energy profiles in Figure 1 discloses that axial complexation of the first C=C bond is favorable in **2** and vital for a facile insertion. To follow the most accessible pathway, cis-1,4 insertion has an intrinsic barrier of 11.4 kcal mol^{-1} (**2a** → **3a**) and is driven by a thermodynamic force that amounts to 10.6 kcal mol^{-1} (**2a** → **2a′**).

Butadiene complexation, to proceed upon displacing the coordinated π-bonds, furnishes **2a′** in a slightly endergonic process (Figure 1). Hence, **1a** appears as the most stable species for strict cis-1,4-enchainment, which is in accord with the absence of butadiene-complexed species as observed by NMR.[10,14]

We have furthermore assessed the likelihood for anti ⇄ syn isomerization through a rotational η^1-C^3-butenyl−Ni^{II} TS structure[20] to commence from **1a** or **2a**. The most accessible pathway is connected to **1a** and is predicted as being kinetically more difficult ($\Delta G^{\ddagger}$ = 20.0 kcal mol^{-1}; Figure 1) than regular cis-1,4-insertion ($\Delta G^{\ddagger}$ = 11.8 kcal mol^{-1}, relative to **1a**, see also Figure 2). The computed $\Delta\Delta G^{\ddagger}$ gap of 8.2 kcal mol^{-1} renders the isomerization as being almost entirely prevented for a strictly cis-1,4-enchained polybutadienyl chain ($k_{2c} \gg k_3$, k_4; Scheme 1). As a consequence, chain growth occurs exclusively through *cis*-butadiene insertion into the *anti*-η^3-butenyl−Ni^{II} group.

Having focused thus far on strict cis-1,4-enchainment, we next considered the influence of a 1,2-insertion event. Experiment identified 1,2-insertion as a rare but viable process with estimated probabilities of about 3:100 (298 K)[11] and 1:100 (243 K)[14] relative to cis-1,4-insertions. Figure 2 summarizes the calculated step profiles for alternative cis-1,4- (**I1a** + C_4H_6 → **I2a** → **I3a** → **I1′a**; see also Figure 1) and 1,2-insertions (**I1a** + C_4H_6 → **I2a** → **II3a** → **II1′a**) (left) and succeeding cis-1,4-insertions after a previous 1,2-insertion. Concerning the aptitude of an *anti*-η^3-butenyl group's C^1 and C^3 centers for C−C bond formation, the substituted C^3 is less reactive and formation of a vinyl group is kinetically disabled relative to regular cis-1,4-enchainment. The computed $\Delta\Delta G^{\ddagger}$ gap of 4.3 kcal mol^{-1} compares reasonably well with experiment.[21] The most stable product species of 1,2 insertion, **II1′a**, bears some similarity to the wrap-around structure of **I1a** (or **I1a′**), where the cis π-bonds from the two preceding 1,4-insertions coordinate equatorially, while the axial vinyl group is noncoordinating. Reduced flexibility of the chain prevents the preferred upright orientation for the first cis π-bond, such that **II1′a** is higher in energy by 12.5 kcal mol^{-1} than the cis-1,4-enchained **I1′a**. Similar to the case for **I1′b**, coordination of the axial (vinyl) double bond, to come at the expense of one of the coordinated cis π-bonds, is highly unfavorable. This is seen from the energetically almost degenerate **II1′b** and **X2** (Scheme 2), having the first or second cis π-bond, respectively, attached, with **X2** being 0.7 kcal mol^{-1} more stable.[19] This led us to conclude that the suggested **X2**[14] (Scheme 2) does not represent the true structure of the resting state.

The first 1,4-insertion following a 1,2-insertion starts with *cis*-butadiene uptake onto the high-energy species **II1′a**. Unsurprisingly, this is driven by a strong thermodynamic force. The intrinsic barrier for insertion is almost identical with what is calculated for strict 1,4-enchainment because of the similar core structures of involved species. This contrasts with the lower stability of the product species **III1′**, which again is owing to some lack of the chain's flexibility to enable the preferred upright orientation of double bonds. The next 1,4-insertion exhibits intrinsic kinetics comparable to that of preceding regular insertion events and leads to **IV1′a**. Species **IV1′a** features a wrap-around structure identical with that of the strictly 1,4-enchained **I1′a**, but with the growing chain attached at the C^3 instead of the C^1 center. DFT predicts that **IV1′a** is the most stable species in the productive polymerization course. Our study is thus in consonance with Brookhart's identification of a vinyl-coordinated polybutadienyl compound as the resting state[14] but also unveils its true structure. Both electronic and steric factors are in operation to account for the difference in stability between

(16) Andrae, D.; Häussermann, U.; Dolg, M.; Stoll, H.; Preuss, H. *Theor. Chim. Acta* **1990**, *77*, 123.

(17) Schäfer, A.; Huber, C.; Ahlrichs, R. *J. Chem. Phys.* **1994**, *100*, 5829.

(18) Calculations employed TURBOMOLE V5.8 and used the TPSS functional together with flexible basis sets of valence triple-ζ quality. See the Supporting Information for full details.

(19) See the Supporting Information for further details.

(20) Tobisch, S.; Taube, R. *Organometallics* **1999**, *18*, 3045.

(21) This transforms into a relative likelihood of ~0.1:100 (298 K) for 1,2- and cis-1,4-insertion events.

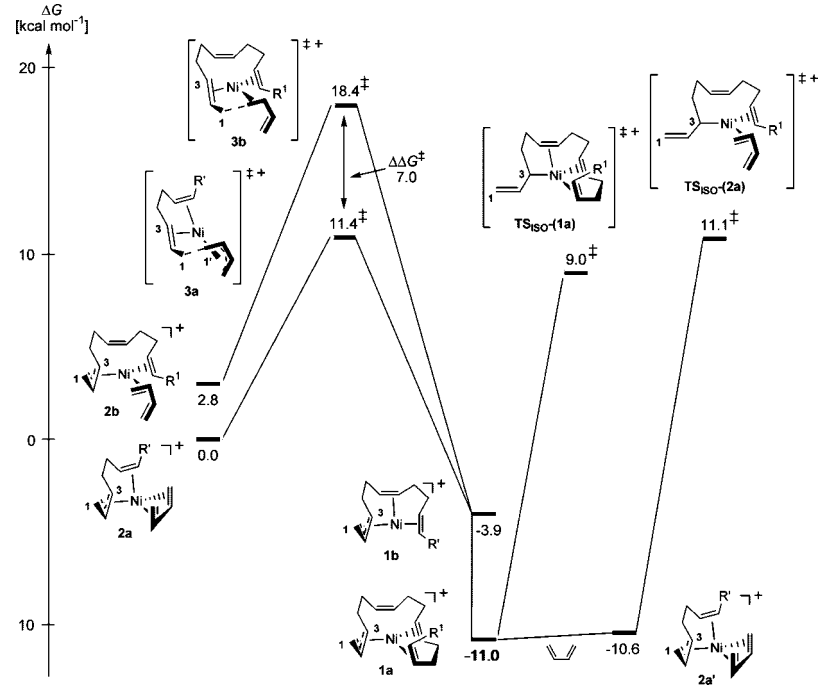

Figure 1. Insertion and allylic isomerization events occurring during strict cis-1,4 enchainment of butadiene by the [(polybutadienyl)-Ni^{II}(*cis*-η^4-butadiene)]$^+$ catalyst species. Calculations employed [(*anti*-η^3-$C_{15}H_{22}R$)Ni^{II}(*cis*-η^4-C_4H_6)]$^+$ (R = CH_3) as a realistic catalyst model. The growing polybutadienyl chain is shortened by a C_4 unit after each insertion event. R′ = $C_8H_{12}CH_3$ and R^1 = $C_4H_6CH_3$.

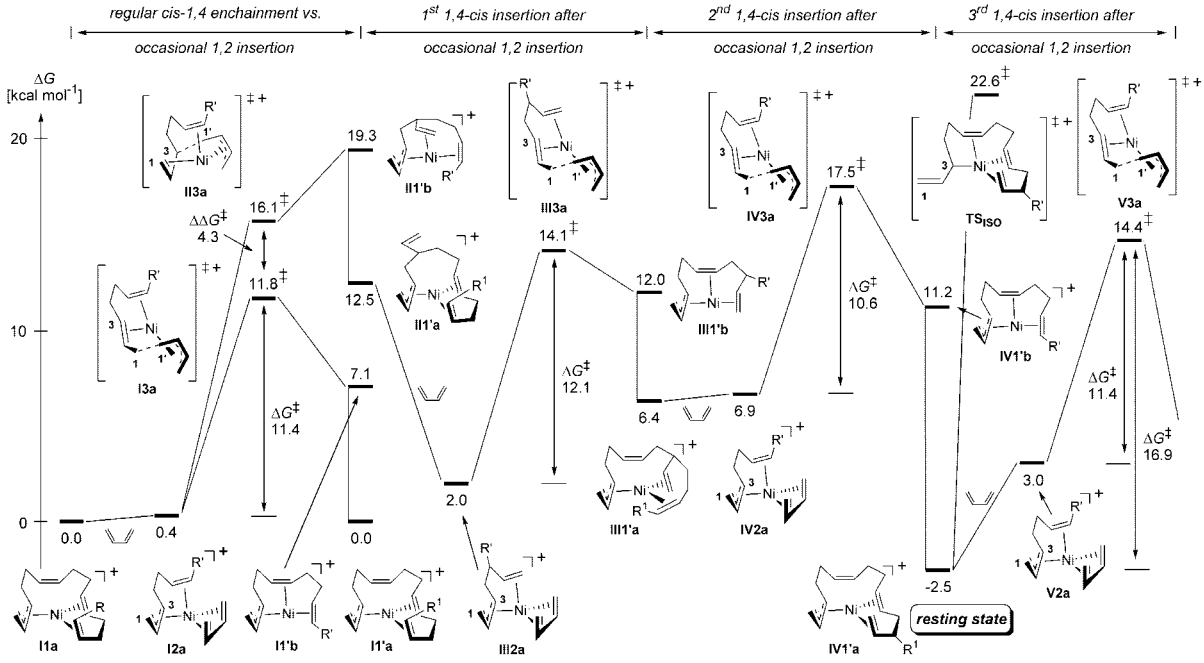

Figure 2. Reaction energy profile for alternative enchainment events of butadiene polymerization by the [(polybutadienyl)Ni^{II}(*cis*-η^4-butadiene)]$^+$ catalyst species (see Figure 1). The calculated reaction heat for regular cis-1,4-enchainment (ΔG = 10.6 kcal mol^{-1}) has been subtracted from insertion products **I1′**, **II1′**, **III1′**, and **IV1′**, respectively. R = CH_3, R′ = $C_8H_{12}CH_3$, and R^1 = $C_4H_6CH_3$.

IV1′a and **I1′a**. On the one hand, **IV1′a** benefits from the better back-bonding abilities of the unsubstituted vinyl group together with rather minor steric encumbrance imposed by the growing chain attached at C^3.

The assignment of **IV1′a** as the true resting state is corroborated further by the calculated ^{1}H NMR spectra of (*cis*-Δ,vinyl)−polybutadienyl−Ni^{II} intermediates **II1′a**,**b**, **III1′a**,**b**, and **IV1′a**,**b** (Table 1, Scheme S1 (Supporting Information)). NMR shielding tensors and vicinal spin–spin coupling constants ^3J are calculated at the TPSS/SDD+TZVP level using the gauge-independent atomic orbital (GIAO) method[22] as implemented in Gaussian 03.[23] The performance of this method, which is known to be reliable,[24] was first tested for **X1** and

(22) (a) London, F. *J. Phys. Radium* **1937**, *8*, 397. (b) Ditchfield, R. *Mol. Phys.* **1974**, *27*, 789. (c) Wolinski, K.; Hinton, J. F.; Pulay, P. *J. Am. Chem. Soc.* **1990**, *112*, 8251. (d) Ruud, K.; Helgaker, T.; Bak, K. L.; Jørgenen, P.; Jensen, H. J. A. *J. Chem. Phys.* **1993**, *99*, 3897. (e) Helgaker, T.; Watson, M.; Handy, N. C. *J. Chem. Phys.* **2000**, *113*, 9402.

Table 1. Calculated and Observed ^{1}H NMR Spectra[a] of (*cis*-Δ,vinyl)−Polybutadienyl−Ni^{II} Intermediates

species	H_{anti}	H_{syn}	H_{cis}	H_{trans}
III1′a	δ 2.76	δ 3.32	δ 5.95[c]	δ 5.61[c]
	$^3J_{H^a-H^1} = 13.2$	$^3J_{H^s-H^1} = 8.0$	$^3J_{H^c-H^b} = 10.8$	$^3J_{H^t-H^b} = 15.7$
III1′b	δ 1.33	δ 2.39	δ 4.37	δ 5.54
	$^3J_{H^a-H^1} = 10.1$	$^3J_{H^s-H^1} = 8.4$	$^3J_{H^c-H^b} = 10.2$	$^3J_{H^t-H^b} = 13.6$
X2	δ 1.79	δ 1.80	δ 6.14	δ 5.65
	$^3J_{H^a-H^1} = 14.0$	$^3J_{H^s-H^1} = 10.3$	$^3J_{H^c-H^b} = 11.0$	$^3J_{H^t-H^b} = 15.4$
III1′a	δ 3.71	δ 5.19	δ 4.43	δ 5.08
	$^3J_{H^a-H^1} = 12.5$	$^3J_{H^s-H^1} = 8.0$	$^3J_{H^c-H^b} = 9.1$	$^3J_{H^t-H^b} = 13.8$
III1′b	δ 2.78	δ 3.66	δ 5.59	δ 5.24
	$^3J_{H^a-H^1} = 10.9$	$^3J_{H^s-H^1} = 8.4$	$^3J_{H^c-H^b} = 9.2$	$^3J_{H^t-H^b} = 15.9$
IV1′a	δ 2.62	δ 3.88	δ 3.37	δ 3.95
	$^3J_{H^a-H^1} = 11.6$	$^3J_{H^s-H^1} = 7.3$	$^3J_{H^c-H^b} = 8.9$	$^3J_{H^t-H^b} = 13.7$
IV1′b	δ 3.14	δ 4.03	δ 5.58[c]	δ 5.68[c]
	$^3J_{H^a-H^1} = 11.4$	$^3J_{H^s-H^1} = 8.2$	$^3J_{H^c-H^b} = 9.6$	$^3J_{H^t-H^b} = 14.3$
exptl resting state[b]	δ 2.94	δ 4.46	δ 3.65	δ 3.95
	$^3J_{H^a-H^1} = 13.5$	$^3J_{H^s-H^1} = 7.5$	$^3J_{H^c-H^b} = 9.0$	$^3J_{H^t-H^b} = 16.5$

[a] Chemical shift δ (ppm) ($\delta = \sigma - \sigma_{TMS}$) and vicinal spin–spin coupling constants ^3J (Hz) are given for protons of the terminal butenyl C^1 center (H_{anti}/H_{syn}) and of the unsubstituted, terminal vinyl group's C^a center (H_{cis}/H_{trans}). See Scheme S1 in the Supporting Information for details. [b] See Figure S3 in ref 14. [c] Noncoordinated vinyl group.

X1m against experimental data[14] and found to be adequate, allowing the semiquantitative prediction of proton chemical shifts and the somewhat less accurate, but still satisfactory, reproduction of coupling constants.[19] This gave us confidence to reassign some of the double-bond protons, thereby demonstrating the predictive value of the computational approach.[19] Of all the various (*cis*-Δ,vinyl)−polybutadienyl−Ni^{II} compounds, the ^{1}H NMR data evaluated for **IV1′a** fits best with the observed NMR fingerprint of the resting state, which conflicts, however, with the previously suggested assignment to **X2**[14] (Table 1). The semiquantitative agreement between observed and calculated NMR data together with the identification of **IV1′a** as being the most stable intermediate in the productive polymerization cycle (Figure 2) provides substantial evidence for **IV1′a** to represent the true resting state.

Since **IV1′a** is the resting state, the next 1,4-insertion determines the observable overall kinetics. This step has an effective barrier of 16.9 kcal mol^{-1} (Figure 2, right). Interconversion of exclusively formed *anti*-**IV1a′** into its syn analogue is significantly slower as the barrier amounts to 22.6 kcal mol^{-1} (Figure 2). In light of the computed kinetic disparity of 8.2 kcal mol^{-1} ($\Delta\Delta G^{\ddagger}$) between alternative insertion and isomerization events ($k'_{2c} \gg k'_3$) in the productive polymerization course it seems unlikely that the k_{2t} route in Scheme 1 accounts for the produced low amount of 1,4-trans polymer. This suggests that the alternative trans-1,4-regulating channel via monoligand butenylnickel(II) compounds is in operation[3] that becomes accessible by a closer associated counteranion to replace the coordinated polybutadienyl chain as the fifth ligand. Experimental support comes from the observation that weakly associating counterions give the highest degree of cis-1,4-enchainment,[11] while the proportion of 1,4-trans polymer increases for more coordinating anions.[3,10h]

To further aid in rationalizing observed activity trends of compounds **X1** and **X1m**, when exposed to butadiene, Figure S3 compares the assessed energetics (see Supporting Information). It shows an identical intrinsic reactivity ($\Delta G^{\ddagger} = 11.4$ kcal mol^{-1} for **2a** → **3a**) for both cases, but the propensity for butadiene uptake is different. The last-coordinated, unsubstituted double bond in **X1** exhibits characteristics similar to those of the vinyl group in the resting state **IV1′a** (Figure 2) and is as such rather difficult to be displaced by butadiene ($\Delta G = 5.5$ kcal mol^{-1}). Reduction of its acceptor strength, together with some steric strain upon 2-Me substitution in **X1m**, causes the uptake to be less endergonic. Hence, the observed higher reactivity of **X1m**, which correlates nicely with the difference in total barriers by 1.4 kcal mol^{-1},[25] is effected entirely by the thermodynamics of butadiene association.

In summary, we have employed the DFT method to fully characterize all relevant elementary steps of 1,3-butadiene polymerization by "ligand-free" polybutadienyl−nickel(II) complexes employing a realistic catalyst model. A detailed view of the chain growth process is presented that aids the correct assignment of spectroscopically observable intermediates. Furthermore, the effective enchainment kinetics has been assessed. Chain growth proceeds through *cis*-butadiene insertion into the *anti*-η^3-butenyl terminal group (π-allyl insertion mechanism),[3,13] where axial coordination of the growing chain's first cis C=C bond is pivotal for facile enchainment. This study is in consonance with the recent NMR identification of a vinyl-coordinated polybutadienyl−Ni^{II} species as the resting state but unveils its true structure as represented by **IV1′a**. The stability of **IV1′a** has been rationalized as originating from the superior back-bonding abilities of the last-coordinated vinyl group, together with minor strain imposed by the growing chain. DFT predicts an effective barrier of 16.9 kcal mol^{-1} ($\Delta G^{\ddagger}$) and $k_p = 2.5$ L mol^{-1} s^{-1} for cis-1,4-enchainment,[26] which is in excellent agreement with experiment ($k_p \approx 3$ L mol^{-1} s^{-1}).[10g] The k_{2t} route (Scheme 1) does not account for the generated low amount of trans-1,4-polymer, which is rather likely to be effected by the alternative trans-1.4-regulating channel via monoligand butenylnickel(II) compounds.[3]

Supporting Information Available: Text giving full details of the employed computational methodology, tables giving computed Cartesian coordinates and energies of all stationary points and additional data given in Schemes S1, S2, and Figures S1−S3. This material is available free of charge via the Internet at http://pubs.acs.org.

OM701214U

(23) Frisch, M. J.; et al. Gaussian 03, Rev. B.05; Gaussian, Inc., Pittsburgh, PA, 2003.

(24) Kaupp, M.; Bühl, M.; Malkin, V. G. *Calculation of NMR and EPR Parameters: Theory and Applications*; Wiley-VCH: Weinheim, Germany, 2004.

(25) This transforms into a relative acceleration by a factor of ~10.

(26) The effective barrier of 16.9 kcal mol^{-1} ($\Delta G^{\ddagger}$) transforms into $k_p = 2.5$ L mol^{-1} s^{-1} by taking the reaction conditions as reported in ref 10g into account.